Correcting Faraday Cup Measurements with Rutherford Backscattering Spectroscopy

Nolan Miles, Joseph Fogt, Trevor Harrison, Hope Weeda, Andrew Bunnell, Paul A. DeYoung, and Kyuil Cho[a)]

Department of Physics, Hope College, Holland, Michigan 49423, USA

[a)]Corresponding author: cho@hope.edu

Abstract. Faraday cups are devices that can measure the intensity of an ion beam by collecting its charged particles. In many accelerator-based studies, the beam intensity must be accurately determined. This requires that a Faraday cup captures all incoming ions and secondary emitted electrons. Instead of constructing a complicated, electrically suppressed Faraday cup, the authors have opted to quantify the systematic error in cup readings with Rutherford scattering at large angles (which is well understood). A proton beam of 3.4 MeV, incident upon a copper target, generated backscattered ions that were captured by a silicon surface barrier detector. This detector measured the energy distribution of the backscattered ions, and the spectrum obtained was used to calculate the current of the ion beam, which could be compared to the simple Faraday cup readings. This comparison produced a correction factor that was used to scale the Faraday cup's measurements to minimize this systematic error.

INTRODUCTION

Many experimental studies in the materials science of semiconductors and superconductors are done by irradiating samples with energetic nuclei. By varying the fluence applied to a sample, one can examine a multitude of properties that are influenced by irradiation, such as amorphism, doping concentration, structural defects, or critical temperature [1, 2, 3]. For these purposes, an accurate measurement of beam fluence is integral to characterizing the effects of irradiating materials. The total fluence can be determined with knowledge of the beam current, beam profile, and the total time of irradiation. Therefore, the beam current must be measured in order to calculate fluence. A Faraday cup is a device that can accomplish this.

A Faraday cup collects ions and, with the addition of a current integrator, measures collected charge over a period of time. The design of Faraday cups is well studied, with much work going into minimizing their sources of systematic error. These include backscattered beam particles and secondary electron emission, which are inherent to their operational mechanism [4, 5]. Various methods, such as manipulating the geometry of the cup to minimize the escape of backscattered particles or utilizing electrostatic fields to recapture emitted electrons, have been shown to reduce these effects [6].

For the purposes of investigating the effects of irradiating superconductive materials, it is important to know the total fluence of the ion beam incident on a sample. This information is useful in quantifying the number of defects induced in the sample. However, one must first know the beam's current in order to calculate fluence. Therefore, the Faraday cup's sources of systematic error must be minimized to obtain the total fluence for a particular measurement. A correction factor is necessary to minimize the deviation of the Faraday cup's measurements from the true beam current. Rutherford backscattering spectroscopy (RBS) is a reliable technique that relates the number of scattered particles to the incident beam intensity.

A simple experimental setup enables one to obtain an RBS energy spectrum that can be compared with a simulated spectrum from the software package Simulation Program for Nuclear Reaction Analysis (SIMNRA) [7] to characterize the beam. In this experiment, an ion beam incident upon a copper target generated backscattered particles that traveled into a silicon surface barrier detector (SSB) [8]. By measuring the geometry of the setup and analyzing RBS data, one can determine the beam current. Therefore, it is integral to this experiment that all of the incoming ions that enter the Faraday cup can also be measured by the SSB detector. This current calculated via RBS can be compared to Faraday cup measurements. From this, a ratio between the RBS current measurement and the Faraday cup's current measurement was determined. The Faraday cup measurements could then be corrected by scaling them by this ratio so that, in future studies, the total fluence for specific irradiations could be correctly calculated with knowledge of the area being irradiated and an accurate beam current.

RUTHERFORD BACKSCATTERING SPECTROSCOPY

The majority of charged particles in an ion beam incident upon a material do not undergo nuclear scattering. Ions that do not backscatter experience inelastic collisions with atomic electrons as they penetrate further into the material, thus reducing their energy until they stop or pass through the target. However, a small fraction of them will collide with nuclei in the material, causing them to backscatter [9, 10, 11, 12]. These interactions are well understood and are well described by models such as Rutherford's differential scattering cross-section for elastic scattering [13].

The authors' main research involves irradiating superconductors with a known fluence. The goal of this work is to determine the true beam current so that this fluence can be accurately determined. In this experiment, a copper target of known thickness (~5 mm) was used for an RBS experiment to determine the beam current. Given the number of particles backscattering at particular energies, the beam current can be calculated using the program SIMNRA [7] by modeling the energy loss of protons as they decelerate into the target. Experimental RBS spectra measured for a 3.4-MeV proton beam incident upon a copper target were imported to SIMNRA and compared with simulated spectra. The experimental data was fit and a typical result is shown in Fig. 1.

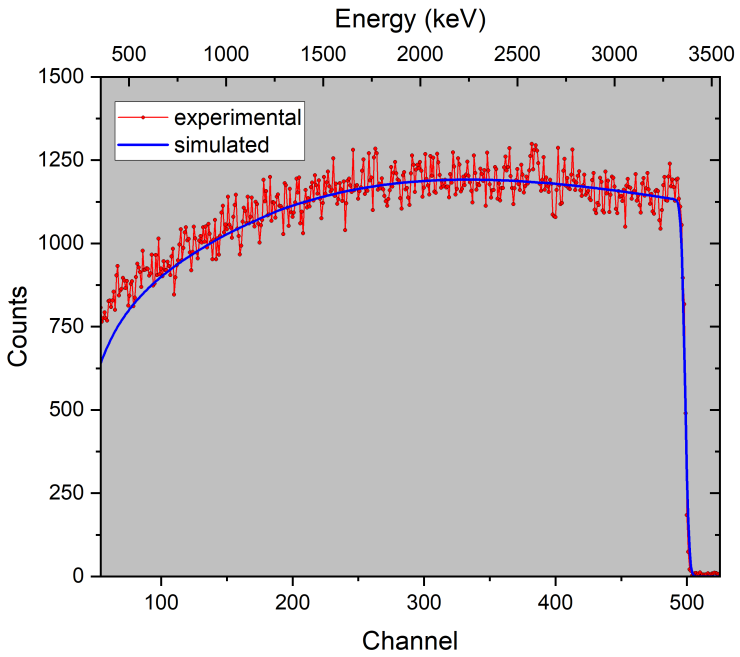

FIGURE 1. Here SIMNRA is employed to model measured energy spectra (Trial 2023.2.8-7), where one (of many) parameters is the number of incident particles independent of any Faraday cup measurements. A single scattering model was used for this fit, which causes the data to diverge from the model at lower energies due to ions experiencing multiple collisions and further depleting their energies.

EXPERIMENTAL SETUP

Hope College's tandem Van de Graaf particle accelerator (NEC 5-SDH) generated a 3.4-MeV proton beam that was directed onto a copper target mounted on a retractable sample holder as shown in Fig. 2. The Ortec SSB detector [14] used in this experiment, having 253 μm thickness and a 5 cm diameter, was positioned at an angle of 168.2° and collimated with a 5-mm-diameter Ta aperture. The signal produced by the SSB detector was conditioned by a Canberra 2003DT preamplifier [15], and the resulting data was histogrammed by a Phillips 7164ADC [16] with a Kmax acquisition system [17]. Due to the collimator's diameter being smaller than the active area on the SSB detector and the low tolerance (approximately $\pm$ 0.005 mm) of the experimental setup, there is minimal error in the

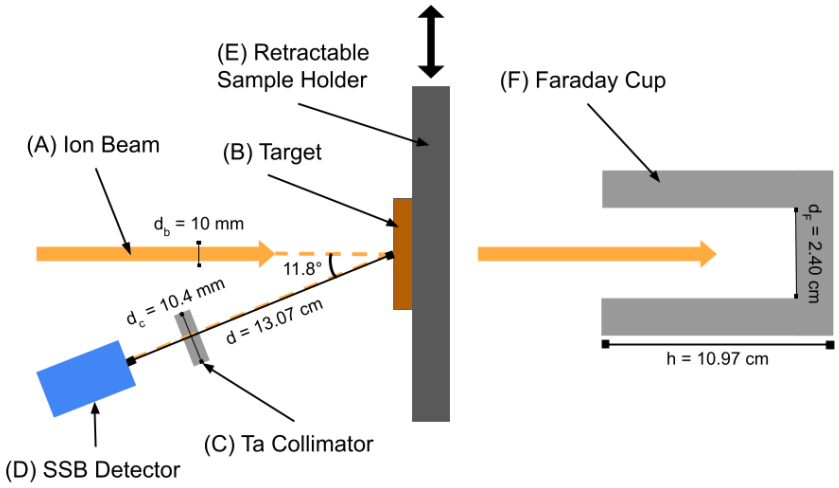

FIGURE 2. Experimental setup diagram where the ion beam (A) interacts with the target material (B), flows through the Ta collimator (C), and the energies of scattered ions are measured by the SSB detector (D). The retractable sample holder (E) can be moved out of the beam's path, allowing the Faraday Cup (F) to catch incoming ions and enabling the beam current to be measured.

SSB detector's angle; therefore, its contribution to the total error of the experiment is negligible. Before irradiating the sample, the ion beam was examined on the beam profile monitor to ensure that its entire cross-sectional area was incident upon the copper target. The beam's energy was kept below the Coulomb barrier to prevent any nuclear reactions from taking place. (There are known isobaric analog resonances populated by the ^{65}Cu(p,n)^{65}Zn reaction that are very narrow and do not produce many neutrons [18]. Standard procedure for this experiment included placing a Bonner sphere neutron detector at the exit of the chamber, and the neutron emission rates never exceeded more than one count per minute.) If there was a measurable deadtime greater than 1%, the beam current was reduced until the deadtime did not exceed 1%. All trials were conducted over three nonconsecutive days between February 1 and February 9, 2023. This experimental schedule ensured that our beam spot was reproducible for each trial and reduced the likelihood of equipment failure between trials.

The RBS data were then analyzed with SIMNRA to obtain the number of incident particles (P). With knowledge of the total time of irradiation (t) and the charge state of the beam particles ($Z = 1$), the RBS current (I_{RBS}) was calculated using Eq. (1), where e is the elementary charge constant. The uncertainty of the I_{RBS} measurements was calculated via propagating the standard error for the number of particles determined by the SIMNRA fit and the total time of irradiation for each RBS experiment:

$$I_{RBS} = \frac{P \cdot e \cdot Z}{t}. \tag{1}$$

Before and after each RBS measurement, the copper-target-sample holder was retracted to allow ions to travel directly into the Faraday cup, enabling the beam current to be measured. The incoming ions were processed by a RedNUN [19] current digitizer, which accumulated charge in intervals of 10^{-11} C to calculate the integrated current. The average of the two measurements was recorded as the average current measured by the Faraday cup (I_{FC}). The uncertainty of the I_{FC} measurements was determined by applying a percent error to the Faraday cup's current measurements relative to average current measurement.

CORRECTION ANALYSIS AND RESULTS

Fitting with SIMNRA was initialized with known experimental parameters such as the energy calibration, the detector location, the detector resolution, the scattering cross-section, the elemental composition, and the thickness of the target. After inputting known parameters, the number of particles was varied until χ^2 was minimized. The value of total incident particles used to fit the experimental spectra enabled the RBS current to be calculated via Eq. (1).

The RBS current values were compared with Faraday cup measurements (Table 1) along with the calculated ratio (I_{FC}/I_{RBS}) between them. Uncertainties were calculated for each ratio by combining the uncertainties in the Faraday cup current measurement ($\pm 3\% \times I_{FC}$) and the fitted number of incident particles ($\pm 5\% \times I_{RBS}$). The weighted average of the ratio across all trials was calculated to be 1.074 ± 0.017. Therefore, the Faraday cup correction factor is 1.074, and all future measurements can be scaled by this amount to yield the true beam current.

TABLE 1. Results from each trial. The current ratio between the RBS and Faraday cup measurements with their associated percentage uncertainties. Each RBS measurement ran for 5 min and the average current measured by the Faraday cup over 1 min was recorded before and after each RBS measurement. The RBS experiment's run length could have been increased to lower the uncertainty in I_{RBS}, but for this experiment, a run length of 5 min yielded acceptable results.

Trial	I_{RBS} (nA)	I_{FC} (nA)	I_{FC}/I_{RBS}
2023.2.1-1	$0.94 \pm 5\%$	$0.99 \pm 3\%$	$1.04 \pm 6\%$
2023.2.1-2	$6.70 \pm 5\%$	$7.12 \pm 3\%$	$1.06 \pm 6\%$
2023.2.1-3	$2.25 \pm 5\%$	$2.45 \pm 3\%$	$1.09 \pm 6\%$
2023.2.8-1	$1.46 \pm 5\%$	$1.54 \pm 3\%$	$1.05 \pm 6\%$
2023.2.8-2	$0.54 \pm 5\%$	$0.59 \pm 3\%$	$1.09 \pm 6\%$
2023.2.8-3B	$1.12 \pm 5\%$	$1.21 \pm 3\%$	$1.08 \pm 6\%$
2023.2.8-5	$0.49 \pm 5\%$	$0.54 \pm 3\%$	$1.09 \pm 6\%$
2023.2.8-6B	$6.25 \pm 5\%$	$6.66 \pm 3\%$	$1.06 \pm 6\%$
2023.2.8-7	$9.81 \pm 5\%$	$10.69 \pm 3\%$	$1.09 \pm 6\%$
2023.2.9-1	$3.98 \pm 5\%$	$4.36 \pm 3\%$	$1.09 \pm 6\%$
2023.2.9-2	$2.30 \pm 5\%$	$2.47 \pm 3\%$	$1.07 \pm 6\%$
2023.2.9-3	$1.26 \pm 5\%$	$1.37 \pm 3\%$	$1.08 \pm 6\%$
2023.2.9-4	$0.84 \pm 5\%$	$0.90 \pm 3\%$	$1.07 \pm 6\%$

CONCLUSION

In conclusion, RBS data were analyzed with SIMNRA to determine the true beam current. The average ratio between the Faraday cup current and the RBS current was determined to be 1.074 ± 0.017. This ratio suggested that the deviation between the Faraday cup measurements and the true beam current was relatively small. This was surprising, considering this is an unsuppressed system. This ratio functions as a correction factor to scale the Faraday cup's current measurements, thus minimizing systematic error. Although this correction factor is sufficient f or ion-beam experiments around 3.4 MeV, its accuracy is diminished at energies much higher or lower than 3.4 MeV. In this experiment, the secondary electron emission was quantified to scale Faraday cup measurements; however, the amount of secondary emissions is not constant across different beam energies. Therefore, the Faraday cup's correction factor is only valid for ion beams around 3.4 MeV. For this reason, future plans include repeating this procedure at a variety of beam energies to develop a correction of the Faraday cup's measurements as a function of energy. The single scattering model employed in SIMNRA produced a slight divergence in the fit at lower energies; however, the overall uncertainty of the I_{RBS} was acceptable for the authors' future work. This improved accuracy will be useful in measuring the beam current directly for the purposes of quantifying the total fluence through a target material in future experiments.

ACKNOWLEDGMENTS

The authors thank Dave Daugherty and Megan Haeussler for their assistance in operating the particle accelerator. This work was supported by the Dean of Natural and Applied Sciences and the Department of Physics at Hope College. The laboratory facilities are supported by the National Science Foundation (NSF). The particle accelerator was funded by NSF Grants No. PHYS-0319523 and No. PHYS-2209138.

Research reported in this publication was supported in part by funding provided by the National Aeronautics and Space Administration (NASA) under Award No. 80NSSC20M0124, the Michigan Space Grant Consortium (MSGC), and the National Science Foundation (NSF).

REFERENCES

1. N. Klein-Kedem, D. Cahen, and G. Hodes, "Effects of light and electron beam irradiation on halide perovskites and their solar cells," Acc. Chem. Res. **49**, 347–354 (2016).
2. B. K. Durant, H. Afshari, S. Singh, B. Rout, G. E. Eperon, and I. R. Sellers, "Tolerance of perovskite solar cells to targeted proton irradiation and electronic ionization induced healing," ACS Energy Lett. **6**, 2362–2368 (2021).
3. J. Fogt, H. Weeda, T. Harrison, N. Miles, and K. Cho, "Effect of proton irradiation on thin-film YBa2Cu3O7- δ superconductor," Materials **17**, 4601 (2024).
4. K. L. Brown and G. W. Tautfest, "Faraday-cup monitors for high-energy electron beams," Rev. Sci. Instrum. **27**, 696–702 (1956).
5. S. Qin, M. P. Bradley, P. L. Kellerman, and K. Saadatmand, "Measurements of secondary electron emission and plasma density enhancement for plasma exposed surfaces using an optically isolated Faraday cup," Rev. Sci. Instrum. **73**, 1153–1156 (2002).
6. E. Cantero, A. Sosa, W. Andreazza, E. Bravin, D. Lanaia, D. Voulot, and C. Welsch, "Design of a compact Faraday cup for low energy, low intensity ion beams," Nucl. Instrum. Methods Phys. Res. A **807**, 86–93 (2016).
7. M. Mayer, "Simnra User's Guide," Report IPP 9/113 (Max-Plank-Institut für Plasmaphysik, Garching, Germany, 1997).
8. S. Gotoh and Z. Takagi, "Silicon surface barrier detector," J. Nucl. Sci. Tech. **1**, 311–315 (1964).
9. H. R. Verma, *Atomic and nuclear analytical methods: XRF, Mossbauer, XPS, NAA and ion-beam spectroscopic techniques* (Springer, Berlin, 2007).
10. E. Rutherford, "LXXIX. The scattering of α and β particles by matter and the structure of the atom," Lond. Edinb. Dubl. Phil. Mag. **21**, 669–688 (1911).
11. A. Nurmela, V. Zazubovich, J. Räisänen, E. Rauhala, and R. Lappalainen, "Elastic scattering cross sections of protons by copper, molybdenum, silver and tin near the Coulomb barrier," J. Appl. Phys. **84**, 1796–1799 (1998).
12. M. Kenny, J. Bird, and E. Clayton, "Proton induced γ-ray yields," Nucl. Instrum. Methods **168**, 115–120 (1980).
13. Y. Maeda, H. Sakai, K. Fujita, M. Greenfield, K. Hatanaka, M. Hatano, J. Kamiya, T. Kawabata, H. Kuboki, H. Okamura, *et al.*, "Differential cross section and analyzing power measurements for n→ d elastic scattering at 248 MeV," Phys. Rev. C **76**, 014004 (2007).
14. "Silicon Charged-Particle Detector Manufactoring," https://www.ortec-online.com/www.ortec-online.com, AMETEK.
15. Canberra Industries, *Preamplifiers: Models 2003BT, 2004, 2005, 2006, 2007B, and 2007P* (2013), product datasheet for charge-sensitive preamplifiers used in nuclear spectroscopy.
16. Phillips Scientific, *Model 7164 16 Channel Peak ADC* (n.d.), technical manual for the Model 7164 analog-to-digital converter.
17. Sparrow Corporation, *Kmax User Manual, Version 11.17* (2023), installation and usage guide for the Kmax cross-platform data acquisition system.
18. S. Saini, G. Singh, A. Chatterjee, S. Kailas, D. Karnik, N. Veerabahu, and M. Mehta, "Isobaric analogue resonances in the 41K and 65Cu (p, n) reactions," Nucl. Phys. A **405**, 55–68 (1983).
19. *RedNUN RN-8111 Charge Pump Digitzer Manual*, Red Nun Instrument Corp., Westfield, New Jersey (1986).